DOI: 10.1002/anie.201408479

Biocomputing

DNA-Programmed Dynamic Assembly of Quantum Dots for Molecular Computation**

*Xuewen He, Zhi Li, Muzi Chen, and Nan Ma**

Abstract: *Despite the widespread use of quantum dots (QDs) for biosensing and bioimaging, QD-based bio-interfaceable and reconfigurable molecular computing systems have not yet been realized. DNA-programmed dynamic assembly of multi-color QDs is presented for the construction of a new class of fluorescence resonance energy transfer (FRET)-based QD computing systems. A complete set of seven elementary logic gates (OR, AND, NOR, NAND, INH, XOR, XNOR) are realized using a series of binary and ternary QD complexes operated by strand displacement reactions. The integration of different logic gates into a half-adder circuit for molecular computation is also demonstrated. This strategy is quite versatile and straightforward for logical operations and would pave the way for QD-biocomputing-based intelligent molecular diagnostics.*

Molecular computation, which mimics conventional microprocessors to perform Boolean functions using elementary logic gates, holds great promise for intelligent biosensing and imaging.[1] Considerable efforts have been made to find good candidates for constructing addressable molecular logic gates for logical operations, through which both non-biological[2] and biomolecular[3] computing systems have been developed. QDs are luminophores that outperform traditional organic fluorophores because of their strong photoluminescence, tunable emission wavelengths, high extinction coefficients, broad excitation ranges, and high photostability.[4] While QDs have been widely applied in biosensing and bioimaging,[5] the use of QDs to construct molecular logic gates for computational applications remains much less explored. The Willner group reported DNA-functionalized QD logic gates based on electron transfer between the QD and specific metal ions chelated in the DNA molecules.[6] The Medintz group reported a QD photonic logic device based on time-gated FRET between a QD, a long-lifetime Tb complex, and a near-IR fluorophore that are assembled through peptide linkers.[7] These studies use either metal ions or artificial fluorophores as inputs, and the electron/energy transfer occurs between QDs and other species. However, fully bio-interfaceable and reconfigurable QD-based molecular computing systems have not been reported to date.

Given that QDs exhibit distinct emission properties in separate and aggregate form as a result of FRET, we envision that a QD computing system could be created by programming the assembly and disassembly of multi-color QDs to manipulate their emission outputs using suitable molecular inputs. In this system, it is expected that the large Stokes shift of QDs could give rise to efficient FRET between closely associated QDs with well-separated emission spectra. Additionally, the simultaneous excitability of multi-color QDs is highly desirable for tracking multiple output signals from integrated logic gates.

Herein, we chose DNA molecules as a platform on which to program the assembly and disassembly of QDs to construct QD computing systems. First, DNA molecules can serve as unique templates to control QD growth, which offers a straightforward strategy to produce DNA-functionalized QDs with precisely tailored DNA valencies for QD assemblies.[8] In particular, the small hydrodynamic sizes of these DNA-functionalized QDs could help minimize the separation distance of QD FRET pairs to ensure efficient FRET. While the static self-assembly of DNA-functionalized QDs for the construction of complex higher-order nanostructures has been demonstrated, the DNA-programmed dynamic and reversible assembly of QDs has not been previously realized. Second, DNA molecules are ideal for logical operations owing to their unique sequence-specific hybridization property and easy programmability.[9] Third, DNA molecules have been universally proven to be able to bind to a variety of biomolecular targets, including nucleic acids, proteins, and cell surface receptors.[8a,10] Thus, DNA-programmed QD computing systems would be potentially generalizable toward various biomolecular targets for biosensing applications.

Herein, we report the DNA-programmed dynamic assembly of multi-color QDs for the construction of QD computing systems. DNA strand displacement, a process in which a single-stranded fuel DNA binds to a partially double-stranded complex by a single-stranded toehold domain and initiates branch migration to displace the pre-hybridized single-stranded DNA,[11] is used to trigger the assembly and disassembly of the QDs. In this study, a complete set of seven binary logic gates (OR, AND, NOR, NAND, INH, XOR, and

[*] X. He, Z. Li, M. Chen, Prof. N. Ma
The Key Lab of Health Chemistry and Molecular Diagnosis of Suzhou
College of Chemistry, Chemical Engineering and Materials Science, Soochow University
199 Ren'ai Road, Suzhou, 215123 (P.R. China)
E-mail: nan.ma@suda.edu.cn

[**] This work was supported in part by the National Natural Science Foundation of China (21175147, 91313302, 21475093), the National High-Tech R&D Program (863 program) (2014AA020518), the Recruitment Program of Global Young Experts (1000-Young Talents Plan), the Project of Scientific and Technologic Infrastructure of Suzhou (SZS201207), the Priority Academic Program Development of Jiangsu Higher Education Institutions (PAPD), and startup funds from Soochow University.

Supporting information for this article is available on the WWW under http://dx.doi.org/10.1002/anie.201408479.

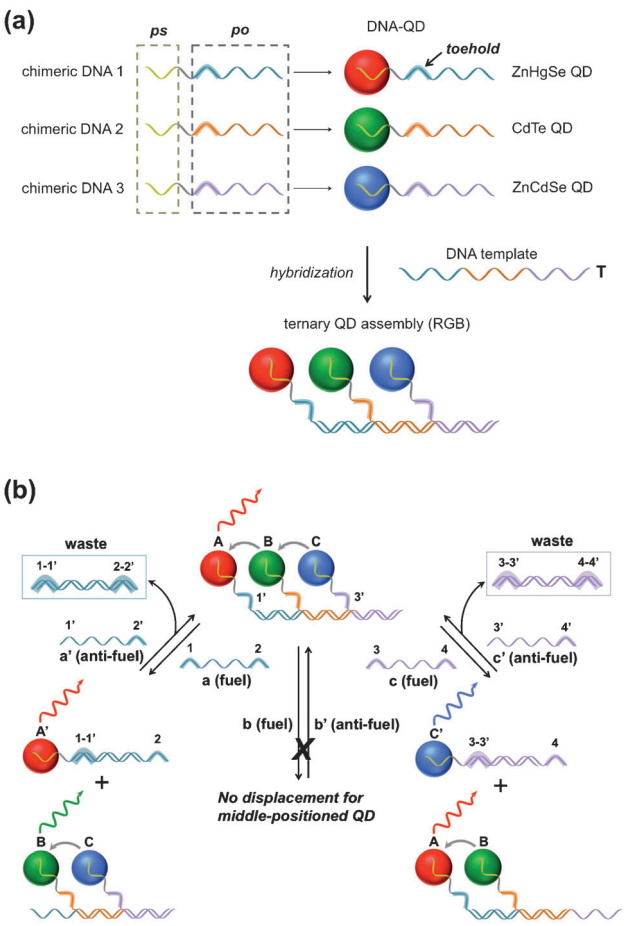

Scheme 1. Illustration of a) construction of ternary QD complex; b) disassembly and reassembly of ternary QD complex through strand displacement reactions.

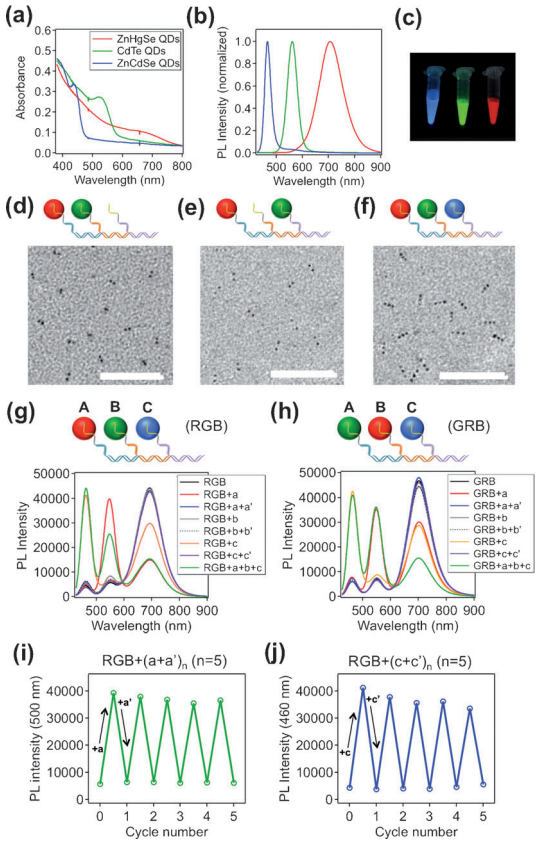

Figure 1. Characterization of DNA-functionalized QDs, assembly, disassembly, and reassembly of the QD complex. a) Absorption spectra, b) normalized PL spectra, and c) PL photograph of the DNA-functionalized ZnHgSe (red), CdTe (green), and ZnCdSe QDs (blue). TEM images of d) RG binary complex (A and B position), e) RG binary complex (A and C position), and f) RGB ternary complex (scale bars are 50 nm in all TEM images). PL spectra of g) RGB and h) GRB ternary complex that have undergone disassembly and reassembly through strand displacement reactions. Multi-round strand displacement reactions of RGB ternary complex with fuel and anti-fuel DNA **a** and **a′** (i); **c** and **c′** (j).

NXOR) is constructed based on dynamic QD assembly. DNA molecules are used as input signals to initiate strand displacement reactions, and the resulting photoluminescence (PL) changes of QDs are monitored as output signals.

First, we construct a ternary QD complex (RGB) by hybridizing three monovalent DNA-QDs with red, green, and blue emissions to DNA template **T** (Scheme 1 a). Three different QDs (ZnHgSe red, CdTe green, and ZnCdSe blue) with comparable PL intensities and well-separated emission spectra are synthesized using three chimeric DNA molecules as ligands. Each chimeric DNA molecule contains a phosphorothioate domain for QD passivation and a phosphate domain for hybridization with the complementary portion of the DNA template **T**. The phosphate domain contains a toehold for the strand displacement reaction. Monovalent DNA-QDs are synthesized following a previously reported procedure.[8a] The mean diameters, emission maxima, and quantum yields (QYs) of the as-prepared red, green, and blue QDs are 4.2 nm/700 nm/36.8 %, 3.8 nm/550 nm/40.3 %, and 3.7 nm/460 nm/64.5 %, respectively (Figure 1; Supporting Information, Figure S1). Efficient hybridization of DNA-QDs with DNA template **T** is confirmed by gel filtration chromatography (GFC; Supporting Information, Figure S2). Uniform and monodisperse binary and ternary QD assemblies could be directly visualized by transmission electron microscopy (TEM) (Figure 1 d–f). The spectral overlap integral $J(\lambda)$ and Förster distance R_0 of each QD FRET pair (comprised of two adjacent QDs in the complex) are calculated to be 9.12×10^{-13} cm^3 M^{-1}/69.2 Å (B–G in RGB), 1.08×10^{-12} cm^3 M^{-1}/65.7 Å (G–R in RGB), and 9.51×10^{-13} cm^3 M^{-1}/69.8 Å (B–R in GRB), respectively. Accordingly, the FRET efficiencies of each QD FRET pair are predicted to be 81.6 % (B–G in RGB), 76.5 % (G–R in RGB), and 82.3 % (B–R in GRB).

To trigger the disassembly of QD **A** from the RGB ternary QD complex, a single-stranded fuel DNA **a** containing two different toeholds (**1** and **2**) at both ends is introduced to initiate the forward strand displacement reaction to displace QD **A** from DNA template **T** (Scheme 1 b). To reassemble QD **A** to DNA template **T**, an anti-fuel DNA **a′** is introduced to react with the fuel DNA **a** associated with the dissembled QD **A** to generate one piece of double-stranded DNA waste, allowing the dissembled QD **A** to be "deprotected" and hybridize with DNA template **T**. As expected, the disassem-

bly of red QD **A** from the RGB ternary QD complex results in a pronounced increase in the PL signal of green QD **B** and a decrease in the PL signal of red QD **A**, indicating that the FRET between QD **A** and **B** is turned off when QD **A** and **B** dissociate from each other (Figure 1g). The FRET between QD **A** and **B** is fully restored when the anti-fuel DNA **a**′ is added to reassemble QD **A** onto the complex. Similarly, the disassembly and reassembly of QD **C** could turn off and turn on the FRET between QD **B** and **C**, respectively (Figure 1g). This reversible assembly process could be performed multiple times (Figure 1i,j; Supporting Information, Figure S3). The strand displacement kinetics could be accelerated by increasing the Mg^{2+} concentration (Supporting Information, Figure S4). Interestingly, the strand displacement reaction is prohibited for the middle-positioned QD **B** in the ternary complex, presumably because of steric hindrance. However, QD **B** could be easily dissembled and reassembled with fuel and anti-fuel DNA (**b** and **b**′) in the binary complex (see below). The ternary QD complex could be constructed with any QD assembly order. For example, we constructed a GRB ternary QD complex with the red QD positioned in the middle. In this case, the disassembly and reassembly of green (blue) QDs increase and decrease the green (blue) PL signals, respectively (Figure 1h).

Next, we constructed a series of binary and ternary QD complexes for DNA-programmed logic gates (Figure 2; Supporting Information, Figure S5). Fuel and anti-fuel DNA are used as input signals to initiate the disassembly and reassembly of QDs, and the output signals are represented by the high (1) or low (0) PL intensity of specific QDs. OR and AND logic gates utilize the disassembly process. The OR logic gate is based on a BG binary QD complex in which the output (blue PL) is 1 if either or both input signals (**a** and **b**) are 1 (Figure 2a; see the Supporting Information, Figure S5 for all the truth tables and PL spectra). The AND logic gate is based on a BGR ternary QD complex in which the output (green PL) is 1 only if both input signals (**a** and **b**) are 1 (Figure 2b). The NOR and NAND logic gates make use of the reassembly process. The NOR logic gate is achieved by reassembling either or both green QD **A**′ and red QD **C**′ onto DNA template **T**, which is pre-assembled with blue QD **B**. It has an output (blue PL) of 1 only if both input signals (**a**′ and **c**′) are 0 (Figure 2c). The NAND logic gate is achieved by reassembling blue QD **A**′ and green QD **B**′ onto DNA template **T**. It has an output (blue PL) of 0 only if both input signals (**a**′ and **b**′) are 1 (Figure 2d). The INH logic gate is realized by the disassembly of the green QD **A** and reassembly of the red QD **C**′ with DNA template **T**, which is pre-assembled with blue QD **B**. It has an output (blue PL) of 1 only if one input signal (**a**) is 1; otherwise, the output is 0 (Figure 2e). The difficult XOR and XNOR logic gates require a more complicated design. For the XOR logic gate, an additional DNA template **T1** was introduced to bind with the dissembled QD **A** and **B** to form a new binary QD complex (Figure 2f; Supporting Information, Figure S5f). This gate has an output (blue PL) of 1 only if the two inputs (**a1** and **b1**) are different (0,1 or 1,0). A similar design is applied for the XNOR logic gate. The blue QD **A** and green QD **B** are pre-assembled onto two different DNA templates **T2** and **T3**. The input DNA (**a1** or **b1**) could disassemble the cognate QD from one DNA template and reassemble it to the other DNA template to form a binary QD complex (Figure 2g; Supporting Information, Figure S5g). This gate has an output (blue PL) of 0 only if the two inputs are different. The output signals of all seven of the logic gates were recorded after two hours incubation (Supporting Information, Figure S6).

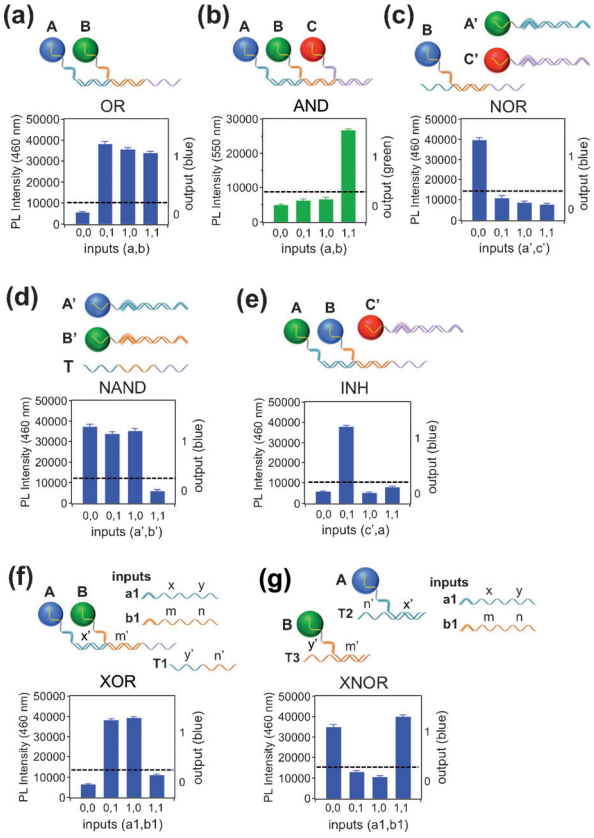

Figure 2. QD photonic logic gates operated by strand displacement reactions. Bar chart presentation of QD PL output signals of a) OR, b) AND, c) NOR, d) NAND, e) INH, f) XOR, and g) XNOR logic gates.

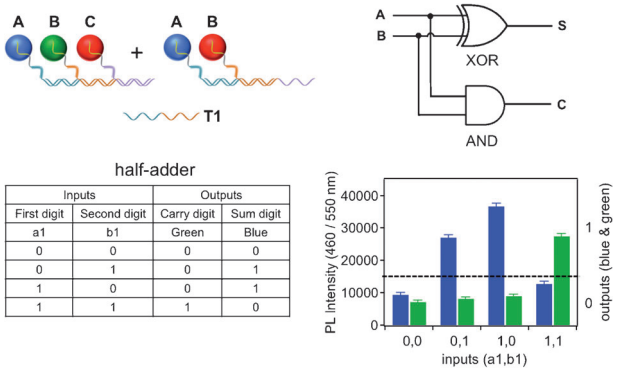

Inputs		Outputs	
First digit	Second digit	Carry digit	Sum digit
a1	b1	Green	Blue
0	0	0	0
0	1	0	1
1	0	0	1
1	1	1	0

Figure 3. Integration of AND and XOR logic gates into a half-adder for molecular computation. Figure shows BGR and BR QD complexes for half-adder construction; the circuitry and truth table of half-adder; and bar chart presentation of QD PL output signals of the half-adder.

Next, we demonstrate the integration of the AND and XOR logic gates to generate a half-adder for molecular computation (Figure 3; Supporting Information, Figure S7). The half-adder adds two single binary digits A and B and has two outputs, the sum (S) digit and carry (C) digit. The sum digit and carry digit are represented by the blue PL and green PL of the QDs, respectively, and can be monitored simultaneously. The carry digit is given by the AND logic gate, and the sum digit is given by the XOR logic gate. A combination of a BGR ternary QD complex and a BR binary QD complex (1:1 molar ratio) is used to construct the half-adder using fuel DNA **a1** and **b1** as inputs.

In summary, we have demonstrated for the first time dynamic and reversible QD assembly controlled by DNA molecules. This dynamic assembly process of QDs is further used to construct a complete set of seven elementary logic gates and an integrated half-adder for molecular computation. To the best of our knowledge, this is the first fully bio-interfaceable and reconfigurable QD molecular computing system. Because of the easy programmability of DNA molecules and the unique optical properties of QDs, the reported strategy is quite versatile for logical operations and shows promise for autonomous intelligent sensing and imaging in the future. For example, the reported QD molecular computing system could potentially serve as an excellent nanoprobe for the logical sensing of biologically relevant nucleic acid molecules (for example, microRNA and mRNA) that act synergistically to determine a disease state. Specifically, the autonomous logic sensors could interact simultaneously with different nucleic acids targets, process information by Boolean logic, and directly make a decision by generating an output light signal, which would open a new avenue for highly efficient and accurate molecular diagnostics for both in vitro and in vivo applications.

Received: August 25, 2014
Revised: September 21, 2014
Published online: October 29, 2014

Keywords: biocomputing · DNA · logic gates · molecular computation · quantum dots

[1] A. P. de Silva, S. Uchiyama, *Nat. Nanotechnol.* **2007**, *2*, 399 – 410.
[2] a) *Molecular Logic-based Computation* (Ed.: A. Prasanna de Silva), The Royal Society of Chemistry, London, **2013**; b) J. Andréasson, U. Pischel, *Chem. Soc. Rev.* **2010**, *39*, 174 – 188; c) G. de Ruiter, M. E. van der Boom, *Angew. Chem. Int. Ed.* **2012**, *51*, 8598 – 8601; *Angew. Chem.* **2012**, *124*, 8726 – 8729; d) S. Erbas-Cakmak, E. U. Akkaya, *Angew. Chem. Int. Ed.* **2013**, *52*, 11364 – 11368; *Angew. Chem.* **2013**, *125*, 11574 – 11578; e) B. Rout, P. Milko, M. A. Iron, L. Motiei, D. Margulies, *J. Am. Chem. Soc.* **2013**, *135*, 15330 – 15333; f) D. S. Kim, V. M. Lynch, J. S. Park, J. L. Sessler, *J. Am. Chem. Soc.* **2013**, *135*, 14889 – 14894.
[3] a) *Biomolecular Information Processing*: *From Logic Systems to Smart Sensors and Actuators* (Ed.: E. Katz), Wiley-VCH, Weinheim, **2012**; b) *FRET—Förster Resonance Energy Transfer*: *From Theory to Applications* (Eds.: I. Medintz, N. Hildebrandt), Wiley-VCH, Weinheim, **2014**; c) M. N. Stojanovic, D. Stefanovic, S. Rudchenko, *Acc. Chem. Res.* **2014**, *47*, 1845 – 1852; d) F. Wang, C.-H. Lu, I. Willner, *Chem. Rev.* **2014**, *114*, 2881 – 2941; e) M. Ikeda, T. Tanida, T. Yoshii, K. Kurotani, S. Onogi, K. Urayama, I. Hamachi, *Nat. Chem.* **2014**, *6*, 511 – 518; f) E. Katz, V. Privman, *Chem. Soc. Rev.* **2010**, *39*, 1835 – 1857; g) M. You, L. Peng, N. Shao, L. Zhang, L. Qiu, C. Cui, W. Tan, *J. Am. Chem. Soc.* **2014**, *136*, 1256 – 1259; h) M. Elstner, J. Axthelm, A. Schiller, *Angew. Chem. Int. Ed.* **2014**, *53*, 7339 – 7343; *Angew. Chem.* **2014**, *126*, 7467 – 7471; i) T. Li, E. Wang, S. Dong, *J. Am. Chem. Soc.* **2009**, *131*, 15082 – 15083; j) X. Feng, X. Duan, L. Liu, F. Feng, S. Wang, Y. Li, D. Zhu, *Angew. Chem. Int. Ed.* **2009**, *48*, 5316 – 5321; *Angew. Chem.* **2009**, *121*, 5420 – 5425.
[4] a) A. P. Alivisatos, *Science* **1996**, *271*, 933 – 937; b) U. Resch-Genger, M. Grabolle, S. Cavaliere-Jaricot, R. Nitschke, T. Nann, *Nat. Methods* **2008**, *5*, 763 – 775; c) X. Michalet, F. F. Pinaud, L. A. Bentolila, J. M. Tsay, S. Doose, J. J. Li, G. Sundaresan, A. M. Wu, S. S. Gambhir, S. Weiss, *Science* **2005**, *307*, 538 – 544; d) I. L. Medintz, H. T. Uyeda, E. R. Goldman, H. Mattoussi, *Nat. Mater.* **2005**, *4*, 435 – 446.
[5] a) M. Bruchez, Jr., M. Moronne, P. Gin, S. Weiss, A. P. Alivisatos, *Science* **1998**, *281*, 2013 – 2016; b) W. C. W. Chan, S. Nie, *Science* **1998**, *281*, 2016 – 2018; c) X. Gao, Y. Cui, R. M. Levenson, L. W. K. Chung, S. Nie, *Nat. Biotechnol.* **2004**, *22*, 969 – 976; d) H. S. Choi, W. Liu, F. Liu, K. Nasr, P. Misra, M. G. Bawendi, J. V. Frangioni, *Nat. Nanotechnol.* **2010**, *5*, 42 – 47; e) I. L. Medintz, A. R. Clapp, F. M. Brunel, T. Tiefenbrunn, H. T. Uyeda, E. L. Chang, J. R. Deschamps, P. E. Dawson, H. Mattoussi, *Nat. Mater.* **2006**, *5*, 581 – 589; f) M. Han, X. Gao, J. Z. Su, S. Nie, *Nat. Biotechnol.* **2001**, *19*, 631 – 635; g) G. Palui, F. Aldeek, W. Wang, H. Mattoussi, *Chem. Soc. Rev.* **2014** DOI: 10.1039/c4cs00124a; h) "Nanocrystals Surface Functionalization": G. Palui, W. Wang, F. Aldeek, H. Mattoussi in *Encyclopedia of Polymer Science and Technology*, Vol. 8, 4th ed., Wiley, Hoboken, **2014**, pp. 785 – 810; i) N. Zhan, G. Palui, M. Safi, H. Mattoussi, *J. Am. Chem. Soc.* **2013**, *135*, 13786 – 13795.
[6] R. Freeman, T. Finder, I. Willner, *Angew. Chem. Int. Ed.* **2009**, *48*, 7818 – 7821; *Angew. Chem.* **2009**, *121*, 7958 – 7961.
[7] a) W. R. Algar, H. Kim, I. L. Medintz, N. Hildebrandt, *Coord. Chem. Rev.* **2014**, *263*, 65 – 85; b) J. C. Claussen, N. Hildebrandt, K. Susumu, M. G. Ancona, I. L. Medintz, *ACS Appl. Mater. Interfaces* **2014**, *6*, 3771 – 3778; c) J. C. Claussen, W. R. Algar, N. Hildebrandt, K. Susumu, M. G. Ancona, I. L. Medintz, *Nanoscale* **2013**, *5*, 12156 – 12170.
[8] a) N. Ma, E. H. Sargent, S. O. Kelley, *Nat. Nanotechnol.* **2009**, *4*, 121 – 125; b) G. Tikhomirov, S. Hoogland, P. E. Lee, A. Fischer, E. H. Sargent, S. O. Kelley, *Nat. Nanotechnol.* **2011**, *6*, 485 – 490; c) N. Ma, G. A. Tikhomirov, S. O. Kelley, *Acc. Chem. Res.* **2010**, *43*, 173 – 180; d) N. Ma, S. O. Kelley, *Wiley Interdiscip. Rev. Nanomed. Nanobiotechnol.* **2013**, *5*, 86 – 95; e) W. Wei, X. He, N. Ma, *Angew. Chem.* **2014**, *126*, 5679 – 5683; *Angew. Chem. Int. Ed.* **2014**, *53*, 5573 – 5577.
[9] a) L. M. Adleman, *Science* **1994**, *266*, 1021 – 1024; b) K. Sakamoto, H. Gouzu, K. Komiya, D. Kiga, S. Yokoyama, T. Yokomori, M. Hagiya, *Science* **2000**, *288*, 1223 – 1226; c) G. Seelig, D. Soloveichik, D. Y. Zhang, E. Winfree, *Science* **2006**, *314*, 1585 – 1588; d) A. Tamsir, J. J. Tabor, C. A. Voigt, *Nature* **2011**, *469*, 212 – 215; e) S. M. Douglas, I. Bachelet, G. M. Church, *Science* **2012**, *335*, 831 – 834; f) X. Chen, A. D. Ellington, *Curr. Opin. Biotechnol.* **2010**, *21*, 392 – 400.
[10] H. Xing, N. Y. Wong, Y. Xiang, Y. Lu, *Curr. Opin. Chem. Biol.* **2012**, *16*, 429 – 435.
[11] D. Y. Zhang, G. Seelig, *Nat. Chem.* **2011**, *3*, 103 – 113.

